PHASE COMPOSITION AND DISPERSITY OF CALCIA STABILIZED ZIRCONIA PRECURSOR, OBTAINED FROM MIXED WATER- 7 VOL.% ACETONE SOLUTION

O.Yu. Kurapova[1,2], M.E. Grega[1], V.D. Somova[1], S.N. Golubev[2] and V.G. Konakov[1,2]

[1]St. Petersburg State University, St. Petersburg, 199034, Russia
[2]Glass and Ceramics Ltd., St. Petersburg, 199004, Russia

Abstract. The work reports the synthesis and of $9CaO-91ZrO_2$ (mol.%) precursor, synthesized by co-precipitation from mixed water-acetone solution. By SEM and adsorption-desorption analysis it was shown that acetone addition acts as cryoprotectant effectively reducing the growth of large hexagonal ice crystals during freeze-drying and results in microporous flakes-like particles. STA analysis showed the decreased crystallization enthalpy comparing to values for powder, obtained from aqueous solution. For the first time the systematic investigation of thermal evolution of agglomerates, crystallites and phase composition of powder obtained from mixed water-7vol.% acetone solution has been performed via PSD and XRD.

1. INTRODUCTION

Nowadays the search of the new routes towards the agglomeration elimination of the ultrafine zirconia based powders is considered the greatest challenge related to the novel ceramic materials development. The agglomeration of nanopowders is very unfavorable but cannot be eliminated completely. As it is mentioned in [1-3] the presence of large and hard agglomerates in precursors lead to the less efficient packing during green bodies compaction and inhomogeneous sintering. So, the microstructure, and, consequently, the values of the anionic conductivity and the mechanical properties of stabilized zirconia ceramics significantly depend on the size and strength of agglomerates in precursors.

It is known that in many cases the agglomerates originate from various stages of synthesis and post-treatment of zirconia based nanosized powders. It was shown that wet chemical techniques are prior to commonly used top-down approaches [4]. The reversed co-precipitation from solutions [5-7], forced hydrolysis at the elevated temperatures [8,9], hydrothermal and solvothermal techniques [10-14] are usually used to manufacture stabilized zirconia powders. A comparative study of various sol-gel methods for zirconia precursors manufacturing was performed in [8]. Among them forced hydrolysis and reversed co-precipitation were especially mentioned. Both of them include a number of variable parameters (as pH, salts concentration temperature, etc.) allowing to obtain ultrafine powders with narrow agglomerate size distribution. It was shown that agglomeration time in solution depends primarily on its viscosity, deposition temperature and initial reagents concentration. The secondary factors affecting the agglomeration are pH, deposition rate and dielectric constant of the solution. In case of co-precipitation and hydrolysis the effects of pH, salts concentration, deposition rate on agglomeration and structure of precursors were investigated rather intensively [15]. Also a sufficient number of works is devoted to the effect of the me-

Corresponding author:O.Yu. Kurapova, e-mail: olga.yu.kurapova@gmail.com

dia in case of hydrolysis [8,9] and solvothermal processes [12-14]. In [9] the spherical ZrO_2 nanoparticles were obtained by heating of the water-alcohol $ZrOCl_2$ solutions (with different content of 1-propanol and 2-propanol). The size of particles and the agglomeration degree was controlled via surfactant addition – hydroxypropyl cellulose. The precipitation mechanism and microstructure are determined by the composition of the solution. Since all surfactants form a film on surface of each particle, their further removal from the powder is quiet challenging. On the other hand, even small residual amount of surfactants can drastically reduce the ionic conductivity of stabilized zirconia ceramics. The similar approach was used in the work [8]. Nanosized zirconia powder was obtained by precipitation from water-alcohol (isopropyl alcohol) of various concentrations. The microspheres with the diameter less 100 nm were obtained via the lowered dielectric constant of solution. However, the choice of medium composition was not clarified. One cannot stand mentioning the patent [16] related to nanosized monodispersed yttria powders formation. Here the precipitation in ammonia aqueous solution was performed in presence of second precipitant – hydrohen peroxide. Yttria powders with the average particle size of 10 to 50 nm were obtained. The approach is original but cannot be applied for various oxides systems. Acetone and ethanol are prospective additions to water as they are completely soluble in water in all the concentrations, form aseotropic solutions and can be easily removed from the gel formed during filtration and dehydration. They can also work as cryoprotectants during freeze-drying [17]. Thus the goal of present work was the study of the disperse medium effect on the agglomeration processes and phase composition at 20-1100 °C.

2. EXPERIMENTAL

2.1. Synthesis

Nanosized $9CaO$-$91ZrO_2$ (mol.%) powder was obtained by reversed co-precipitation from diluted aqueous-acetone salt solution. Nitrate hydrates $ZrO(NO_3)_2 \cdot 2H_2O$ and $Ca(NO_3)_2 \cdot 2H_2O$ were used to prepare 0.1M water-acetone solution containing 7 vol.% of acetone. 1M ammonia aqueous solution was used as a precipitant. Mixed salt solution was added to NH_4OH by drops with a rate of ~ 2 ml/min. The precipitation has been performed at ~1-2 °C in an ice bath at the constant stirring; pH of the solution was kept at ~9-10 during the synthesis by means of ammonium solution addition. To remove reaction byproducts, the obtained gels were filtered and rinsed until the neutral pH was reached. Thus obtained gels underwent freeze-drying (Labconco, 1l chamber, USA 0.018 Torr, 20 °C, 24 hours).

2.2. Analysis

Microstructure of sample after the synthesis was investigated by scanning electron microscopy (SEM, Hitachi S-3400N, accelerating voltage 20 kV). The data on precursor specific surface area was obtained using adsorption-desorption technique (ASAP 2020MP Micromeritics). Simultaneous thermal analysis (STA, STA 449 F1 Jupiter Netzsch, nitrogen ambience, the heating velocity 10 deg./min.) was performed in order to investigate phase transition temperature. Phase composition of precursor after synthesis and thermal treatment in the range 400-1100 °C was identified using X-ray diffraction analysis (XRD, Shimadzu XRD-6000, Cu-Kα radiation, λ = 1.54 Å, room temperature). The mean size of crystallites was estimated via Scherrer's equation using the profile of the peak at 2θ=29.5°.

3. RESULTS AND DISCUSSION

The microstructure of the precursor after synthesis and freeze-drying is shown in Fig. 1. As it is seen from SEM microphotograph (see Fig. 1a), the microstructure of powder considerably differs from sponge-like porous network, which is typical for oxide powders after freeze-drying. Precursor obtained from mixed water-acetone solution consists of the agglomerated flakes with low open porosity. Acetone, likely, acts as a cryoprotectant that reduces the growth of large hexagonal ice crystals during freezing and freeze-drying. The assumption is in accordance with adsorption-desorption data. As seen from Fig. 1b, the microstructure of precursor is microporous. Rather small hysteresis loop indicates that the porosity is only due to free space left between closely packed powder particles. Specific surface area calculated from adsorption-desorption data is 110 m^2/g. That value is significantly lower comparing to literature data on freeze-dried stabilized zirconia powders, obtained from aqueous solutions (i.e. 180-200 m^2/g). It is probably due to flake-shape of the particles obtained. So, the addition of 7 vol.% of acetone to water prior to co-precipitation significantly changes precursor microstructure and decrease its specific area.

STA data for the precursor is presented in Fig. 2. Two effects are present in the DSC curve of the sample. The endothermic effect taking place at 20–
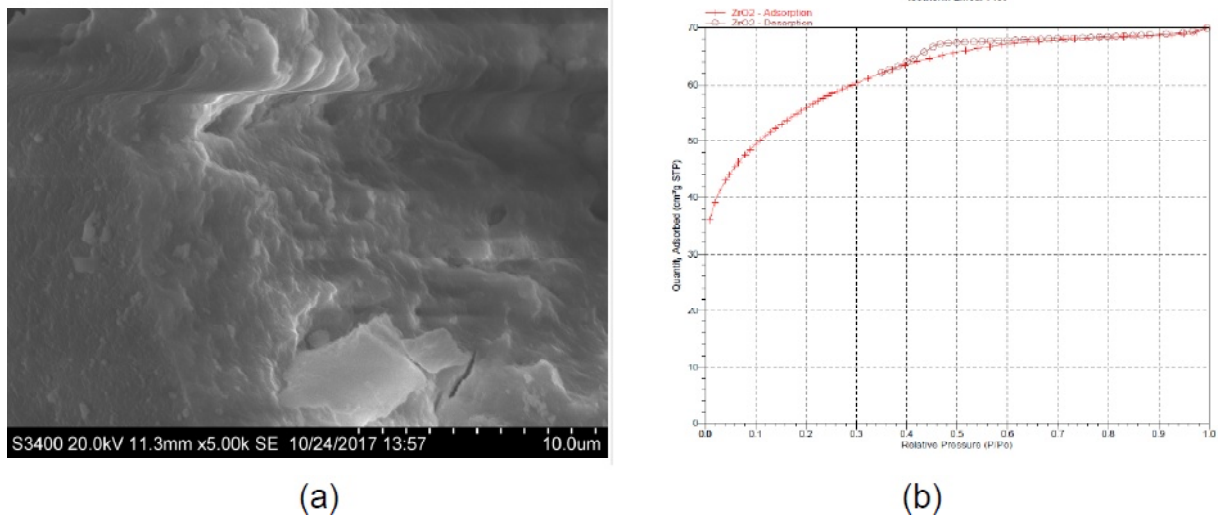
(a)   (b)

Fig. 1. Microstructure of the precursor after synthesis from 93water-7acetone solution (vol.%) (a) SEM data, (b) adsorption-desorption data.
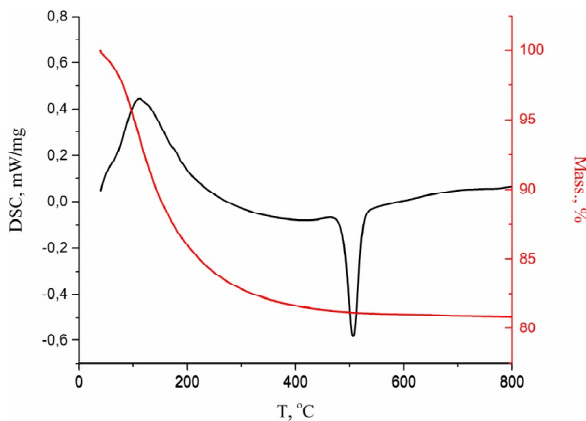

Fig. 2. STA data for 9CaO-91ZrO$_2$ (mol.%) precursor obtained from water-7 vol.% acetone solution.

280 °C corresponds to water losses and the exothermic one at 487 – 513 °C corresponds to crystallization.

Large endothermic peak with the maximum at 112 °C indicates prolonged losses of structural and dispersed water, which is confirmed by TG analysis. Indeed, water losses at the region 20-400 °C calculated from TG curve are 18.95 % (see Table 1). Comparing the obtained value of the mass losses with data of [18,19] for freeze-dried powder and hypothetic composition consisted of hydroxides

9Ca(OH)$_2$-91Zr(OH)$_4$ (24.8 and 26.49, mass.% respectively) one can see, that water in precursor is present in a form of OH-groups. Residual acetone in washed gel, most probably forms azeotrope with water and freeze-drying takes place faster and more efficient.

Table 1 lists the data on phase transitions obtained from DSC and TG curves together with mean agglomerate size in precursor powder after synthesis. Phase transition temperature of powder is slightly shifted towards higher temperatures comparing to freeze-dried powder, obtained from aqueous solution. At the same time crystallization enthalpies differ in ~2 times i.e. -78.7 and -162.2 J/g [19] for powder freeze-dried with acetone addition and without, respectively. The difference in crystallization completeness can be understood upon the detailed consideration of the evolution of phase composition, crystallite size and crystallinity of powder in the range 200-1100 °C.

XRD patterns of precursor annealed at different temperatures are shown in Fig. 3. As it is seen from Fig. 3a, 9CaO-91ZrO$_2$ (mol.%) precursor after the annealing at 400 °C is amorphous. However, the increased intensity at 2θ=29.5° indicates the presence of primary crystallites in the powder. Further

Table 1. Water losses, temperatures, and enthalpies of endo- and exothermal effects, calculate from STA data and mean agglomerate powder size according to PSD-analysis.

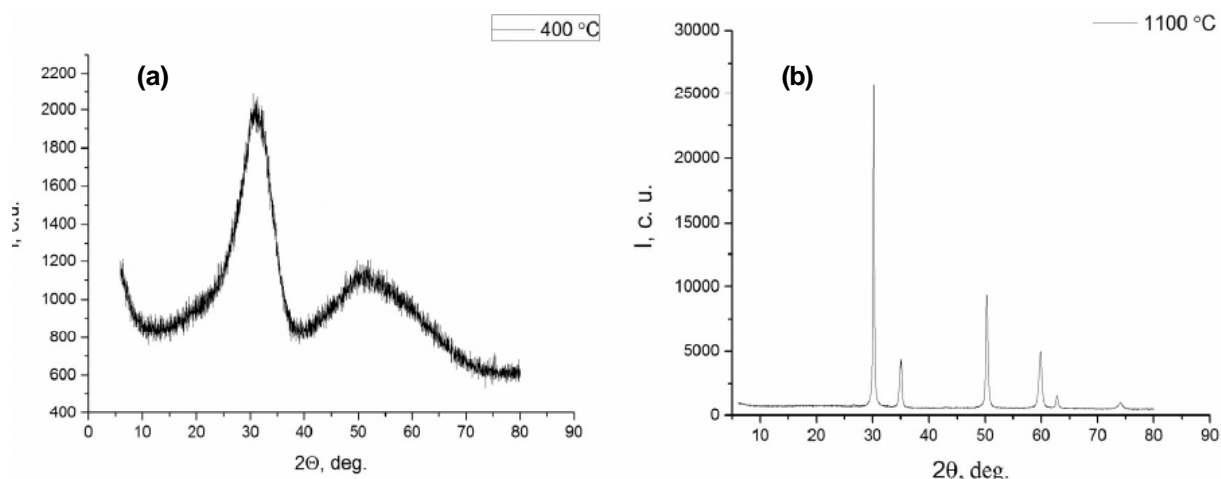| Mass losses T<400 °C, mass. %	$T_{dehydation}$, °C	$T_{crystallization}$, °C	$\Delta H_{dehydtation}$, J/g	$\Delta H_{crystallization}$, J/g	d, nm
18 .95	112 .3	506 .4	297 .3	-78 .7	930

Fig. 3. XRD pattern of 9CaO-91ZrO$_2$ (mol.%) precursor obtained from 93water-7acetone (vol.%) solution and annealed at (a) 400 °C, 2 hours; (b) 1100 °C, 2 hours.
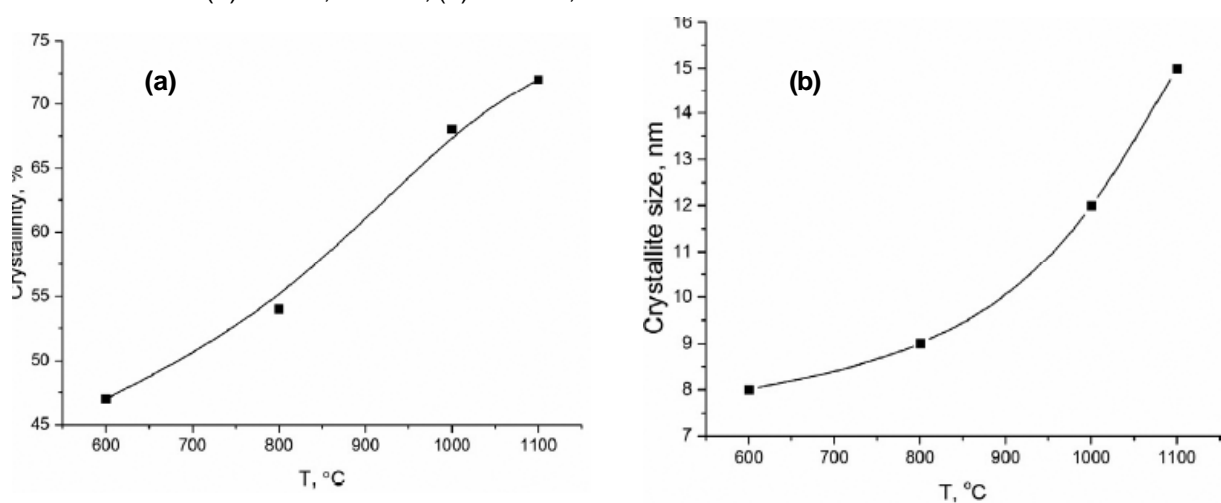

Fig. 4. Dependence of (a) crystallinity and (b) crystallite size on the treatment temperature, in 9CaO-91ZrO$_2$ (mol.%) precursor obtained from water-7 vol.% acetone solution.

annealing at temperatures, higher then phase transition "amorphous phase → crystalline phase" results in metastable cubic zirconia solid solution formation without admixtures of low-symmetric modifications in all investigated region i.e. 600-1100 °C (see Fig. 3b). Since the difference in the obtained XRD patterns is just in the peaks intensity, the crystallite size and crystallinity values were evaluated from XRD data. The dependencies of crystallinity and crystallite size on the treatment temperature are presented in Fig. 4.

From Figs. 4a and 4b it is seen that both crystallinity and crystallites size increase with the temperature of annealing. At 1100 °C crystallinity reaches 73%, i.e. cubic solid solution is well formed. Crystallites are nanosized in all investigated region, which is, likely, one of the factors providing stability of metastable cubic zirconia based solid solution. Notable, that crystallite size in powder is already 8 nm at 600 °C. Probably, primarily crystallites are

formed during freeze-drying with acetone, facilitating crystallization and decreasing crystallization enthalpy. High dispersity of powders is regarded as one more stabilization factor for metastable zirconia phases [1-3]. For that, agglomerate size distribution was obtained for powders after synthesis and annealing at different temperatures via PSD-analysis. Ultrasound was used to determine the agglomerate strength. Mean agglomerate size was calculated for all samples with and without ultrasound treatment. Fig. 5 shows the mean agglomerate size dependence on thermal treatment temperature and ultrasound impact.

From Fig. 5 one can see that the shape of the curves is rather similar to the temperature dependence of agglomerates for freeze-drying of gels, obtained from aqueous solution [18,19]. The agglomerates are soft and can broken by mechanical impact (ultrasound). In general two regions can be distinguished in curves i.e. deagglomeration at 20-800 °C
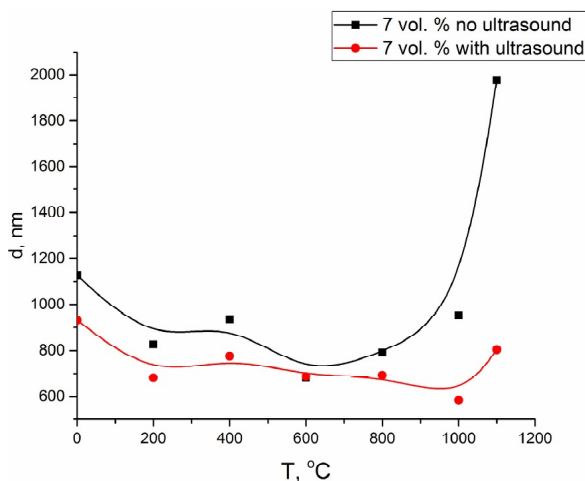
Fig. 5. Dependence of mean agglomerate size on thermal treatment temperature of 9CaO-91ZrO$_2$ (mol.%) precursor with and without ultrasound treatment.

or even 1000 °C and then particles baking. It should be noted that the Dehydration and crystallization processes cause slight agglomerate size decrease with temperature. Slight change of mean agglomerate size with treatment temperature is, likely, due to rather small amount of residual water in powder, not profound crystallization effect and slow growth of crystallites at 600-800 °C (see Fig. 4b). It is important to note that even at 1100 °C the baking of agglomerates is not active. Agglomeration of particles takes place instead. Indeed, ultrasound impact results in ~2.8 times mean agglomerate size decrease from 1970 to 810 nm, which can be explained from the positions of flake-like microstructure of powders obtained.

4. CONCLUSIONS

Via SEM and adsorption-desorption technique it was shown that precursor obtained from mixed water-acetone solution is microporous consisted of flake-like agglomerates. The existence of metastable cubic zirconia based solid solution with no low-symmetric phase admixture up to 1100 °C is due to nanosized crystallites and high powders dispersity. By PSD-analysis it was demonstrated that deagglomeration of particles takes place up to 1000 °C. At higher 1000 °C agglomeration prevails over the baking of agglomerates.

ACKNOLEDGEMENTS

REFERENCES

[1] R. Stevens, *Zirconia and zirconia ceramics* (Magnesium Electron Ltd, 1986).

[2] B.G. Lindsten, *The structure and properties of adsorbents and catalysts* (Mir, Moscow, 1973).

[3] J. Mouzon and M. Oden // *J. Amer. Cer. Soc.* **89** (2006) 3094.

[4] B. Bhushan, *Springer Handbook of nanotechnology* (Spinger-Verlag Berlin Heidelberg New York, 2004).

[5] A. Brune, M. Lajavardi, D. Fisler and J.B. Wagner // *Solid State Ionics* **106** (1998) P.89.

[6] H.J. Schmidt // *Sol Gel Sci. Technol.* **40** (2006) P.115.

[7] S. Shukla, S. Seal and R. Vanfleet // *J Sol Gel Sci. Technol.* **27** (2003) 119.

[8] M. Z.-C. Hu, R. D. Hunt, E. A. Payzant and C. R. Hubbard // *J. Am. Ceram. Soc.* **82** (1999) P.2313.

[9] Y. T. Moon, H. K. Park, D. K. Kim and C. H. Kim // *J. Am. Ceram. Soc.* **78** (1995) 2690.

[10] K. Tsukada, S. Venigalla and A.A. Morrone // *J. Amer. Cer. Soc.* **5** (1999) 1664.

[11] K. Zhu, D.Yang and L. Zhu // *J. Amer. Cer. Soc.* **90** (2007) 1334.

[12] J. Becker // *ACS nano* **2** (2008) 1058.

[13] J. Zhao // *Journal of Materials Research* **15** (2000) 402.

[14] M. Distaso, D. Segets, R. Wernet, R. K. Taylor and W. Peukert // *Nanoscale* **4** (2012) P. 864.

[15] O.Yu. Kurapova and V.G. Konakov // *Rev. Adv. Mater. Sci.* **36** (2014) 176.

[16] G.B. Telnova, A.S. Policarpova and K.A. Solntsev, *patent* **RU 2354610**, (2009).

[17] O. Yu. Kurapova, V.G. Konakov, S.N. Golubev and V.M. Ushakov // *Bull. SpbSU Ser. 4*, **3** (2013) 72.

[18] O.Yu. Kurapova, D.V. Nechaeva, A.V. Ivanov, S.N. Golubev, V.M. Ushakov and V.G. Konakov // *Rev. Adv. Mater. Sci.* **47** (2016) 96.

[19] O.Yu. Kurapova, S.N. Golubev, V.M. Ushakov and V.G. Konakov // *Rev. Adv. Mater. Sci.* **48** (2017) 147.